J. exp. Biol. **154**, 45–65 (1990)
Printed in Great Britain © *The Company of Biologists Limited 1990*

CHARACTERISTICS OF FIVE TYPES OF K^+ CHANNEL IN CULTURED LOCUST MUSCLE

BY B. A. MILLER AND P. N. R. USHERWOOD

Department of Zoology, University of Nottingham, University Park, Nottingham NG7 2RD, UK

Accepted 3 July 1990

Summary

K^+ channel activity in cultured locust myofibres was investigated using gigaohm patch-clamp techniques. After 2 months *in vitro* the myofibres had a mean resting potential of -39 ± 7 mV ($\pm$S.D., $N=42$). Five types of K^+ channel were identified at this time. The majority of single-channel events recorded from cell-attached patches were due to a small-conductance (type 1) and a large-conductance (type 2), inward rectifier, K^+ channel. In cell-attached patches, with 180 mmol l^{-1} KCl in the patch pipette, the type 1 channel had a chord conductance of 43 pS for inward currents and 8 pS for outward currents; the type 2 channel had a chord conductance of 115 pS for inward currents and 29 pS for outward currents. The type 2 channel exhibited bursting kinetics, was ATP-sensitive and could be blocked by Ba^{2+}. Two other channels (types 3 and 4) had linear conductances of 130 pS and 207 pS, respectively. The type 3 channel was Ca^{2+}-sensitive. A further channel (type 5) appeared to be an inward rectifier with a conductance of 5 pS. Openings of types 3, 4 and 5 channels occurred less frequently than openings of the other two channels. Types 1, 2, 3 and 4 channels possessed multiple closed and open states with non-linear gating mechanisms.

Introduction

Studies of voltage-sensitive K^+ currents have revealed a diversity of K^+ channels which are present in the membranes of many cell types and which frequently co-exist in the same membrane. Single-channel conductances range from the 2 pS delayed rectifier of snail (*Helix pomatia*) neurones (Lux *et al.* 1981) to the 250 pS maxi-K^+ channel found in rabbit sarcoplasmic reticulum (Latorre, 1986). K^+ channels differ from one another in their current–voltage (I–V) relationships, gating kinetics, structure, pharmacology and function (for reviews see Latorre and Miller, 1983; Rudy, 1988; Kolb, 1989).

Particularly detailed studies of K^+ channels have been undertaken in insect muscle, both *in vivo* and *in vitro*, using the dorsal longitudinal flight muscles of larval and adult *Drosophila melanogaster*. Studies of wildtype and mutant individuals have disclosed several types of K^+ current. First, a Ca^{2+}-sensitive,

Key words: cultured muscle, K^+ channel, patch-clamp, *Schistocerca gregaria*.

depolarisation-activated, transient, K^+ current (I_A) which exhibits rapid activation and inactivation kinetics (Salkoff, 1983; Salkoff and Wyman, 1983; Wu *et al.* 1983). This current is present in both adult *Drosophila* and cultured myotubes (Solc *et al.* 1987; Wu and Ganetzky, 1988; Zagotta *et al.* 1988). A K^+ channel with a conductance of 14 pS has been shown to be responsible for the I_A current in *Drosophila* myotubes (Zagotta *et al.* 1988). Second, an outward K^+ current (I_K), exhibiting slow inactivation, which appears in adult *Drosophila* muscle at about 96 h post-pupation. This I_K current is also present in cultured myotubes after 16 h *in vitro*. Two K^+ channels, designated K_D (14 pS) and K_O (40 pS), contribute to this current, with the K_D channel contributing the largest fraction (Zagotta *et al.* 1988). Third, a Ca^{2+}-dependent K^+ current (I_{KCa}) found in the muscles of third-instar *Drosophila* larvae. Fourth, a Ca^{2+}-activated K^+ current (I_{Acd}) found in the dorsal longitudinal flight muscles of adult *Drosophila*, which becomes active after I_{KCa} matures in young adults. This current exhibits steady-state inactivation kinetics and is blocked by Ba^{2+} (Wu, 1988; Wu and Ganetzky, 1988). Fifth, a stretch-sensitive K^+ channel (90 pS), designated K_{ST}, which is present in myotubes and is voltage- and Ca^{2+}-independent (Zagotta *et al.* 1988).

K^+ and Cl^- are responsible for the resting membrane permeability of locust skeletal muscle. The concentration gradients of these ions are maintained by metabolic pumps (Usherwood, 1967, 1969; Piek and Njio, 1979; Pichon and Ashcroft, 1985; Leech, 1986). Depolarisation of the locust muscle fibre leads to a voltage-dependent increase in the Na^+ permeability, possibly accompanied by an increase in Ca^{2+} permeability and a delayed increase in K^+ permeability (Usherwood, 1969). Current–voltage studies of the locust retractor unguis muscle undertaken in environments with varying K^+ concentrations reveal the presence of inward and delayed rectifying K^+ currents (Usherwood, 1969). The following is a report on the voltage-sensitive K^+ channels present in cultured locust muscle.

Materials and methods

Primary cultures of locust skeletal muscle

Primary cultures containing skeletal myofibres were prepared from eviscerated, mechanically dissociated 11- to 12-day-old embryos of the locust *Schistocerca gregaria*. The cells were plated out in '5+4' medium (Chen and Levi-Montalcini, 1969) using a modified version of the hanging-column technique (Shields *et al.* 1975). Cultures were incubated in a humidified atmosphere at 28°C. Full details of the methodology are contained in a paper by Duce and Usherwood (1986).

Patch-clamp recording

Locust muscle cultures were used for single-channel studies employing giga-ohm patch-clamp techniques (Hamill *et al.* 1981). Recordings were made in the cell-attached, inside-out and outside-out modes. For the recordings the growth medium was replaced by standard locust saline [180 mmol l^{-1} NaCl; 10 mmol l^{-1} KCl; 2 mmol l^{-1} $CaCl_2$; 3 mmol l^{-1} Hepes buffer, pH 6.8; Usherwood and

Grundfest (1965)]. The culture dish was placed on the stage of an inverted, phase-contrast microscope with a long-range condensor (Olympus C.K.). The indifferent electrode, a Ag/AgCl wire, was immersed in the saline and connected to the headstage of the patch-clamp amplifier (List LM-EPC7). All experiments were conducted at room temperature (20–24°C).

Patch pipettes, made from micro-haematocrit tubing (Hawksley and Sons Ltd), were pulled in two stages using a vertical microelectrode puller (Kopf Instruments, model 700C). Pipettes with a broad shaft and a fine tip were used, with resistances in the 3–8 MΩ range when filled with saline. The tips and shoulders of the pipettes were coated with Sylgard resin (Dow Corning). The pipettes were filled with a high-K^+ saline in which the concentrations of Na^+ and K^+ in the standard saline were reversed, i.e. the pipette saline contained 180 mmol l^{-1} KCl and 10 mmol l^{-1} NaCl.

Currents were recorded on a video cassette recorder (Sony β-max S1 F30) using a pulse-code modulation unit (PCM 701 ES) modified to give a uniform frequency response from d.c. to 20 kHz (Lamb, 1985).

Analysis of single-channel data

Data were low-pass filtered at either 3 or 10 kHz using a Tektronix differential amplifier. Data reduction was undertaken using a MassComp MC5500 computer system, using procedures which are standard in our laboratory (Kerry *et al.* 1987*a–c*; Ball and Sansom, 1988). For analysis, the data were digitised at intervals of 50 μs (20 kHz) for current amplitude analysis and at intervals of 20 μs (50 kHz) for dwell time analysis. The reduced data were stored on hard disc.

Amplitude measurements of single-channel currents

For every 50 μs sample point of the digitised data the amplitude of a channel current (pA) was calculated and used to construct frequency histograms. Gaussian distributions were fitted to the frequency histograms using a non-linear least-squares algorithm (NAG subroutine E04FDF), the means of which were taken to represent the currents of the closed and open states of the channel. The probability of a channel being in its open state (P_o) was determined from the integral of the points lying under the curves.

Calculation of the gating charges

The gating charge was calculated using the Boltzmann equation (Hille, 1984). If a channel has two states, closed and open, then the transition from closed to open can be considered to be a conformational change that moves a gating charge of valence (z) from the inner to the outer membrane surface across a membrane potential difference E. If w represents the conformational energy increase upon opening the channel when E is 0 mV, then the increase of electrical energy in opening the channel with an imposed membrane potential is $-zeE$, where e is the elementary charge, i.e. 1.602×10^{-19} C. Therefore, the total energy change can be expressed as $(w-zeE)$. The Boltzmann equation can be rewritten to define the

ratio of open to closed channels at equilibrium in terms of their energy change and this then gives the voltage dependence of gating of the system:

$$\frac{P_o}{P_c} = \exp - [(w - zeE)/KT] . \quad (1)$$

P_o and P_c are the respective probabilities that the channel will be in either its open or its closed state, K is a kelvin and T is absolute temperature. Rearranging equation 1 gives:

$$P_o = 1/\{1 + \exp[(w - zeE)/KT]\} . \quad (2)$$

If $E_{1/2}$ is the potential where P_o is 0.5, then equation 2 can be written:

$$0.5 = 1/\{1 + \exp[(w - zeE_{1/2})/KT]\} , \quad (3)$$

which gives:

$$w = zeE_{1/2} .$$

Putting this back into equation 2:

$$P_o = 1/\{1 + \exp[ze/KT(E_{1/2} - E)]\} . \quad (4)$$

This gives:

$$\ln[(1 - P_o)/P_o] = ze/KTE_{1/2} - ze/KTE . \quad (5)$$

When $\ln[(1-P_o)/P_o]$ is plotted against E, the intercept is $ze/KTE_{1/2}$ and the slope is $-ze/KT$. These values can then be used to calculate the values of z and $E_{1/2}$.

Analysis of the channel dwell times

Channel dwell times were measured using a single cursor set halfway between the closed and open channel current levels of the digitised data (Colquhoun and Sigworth, 1983). Any open-state transitions which crossed this half-amplitude threshold were detected. Open and closed events longer than 60 μs were readily recognised using this approach.

Dwell time distributions were expressed as histograms. These histograms were normalized to give estimates of dwell time probability density functions (PDFs) (Colquhoun and Sigworth, 1983). Dwell time PDFs providing information on the number of open and closed states of the channel (Fredkin *et al.* 1985; Ball and Sansom, 1987; Kerry *et al.* 1987*a*) were displayed on logarithmic plots (Blatz and Magleby, 1986). To include channel dwell times ranging over several orders of magnitude, the bin widths were exponentially increased (Kerry *et al.* 1987*b*). The dwell time PDFs were fitted with one or more exponential functions using a simplex algorithm (NAG subroutine E04CCF), which used a method of maximum likelihood to determine the most probable parameters for the proportion (α) and the time-constant (τ) of each exponential component. These initial fits were then optimized using a Gauss–Newton–Marquardt algorithm (Marquardt, 1963; Kerry *et al.* 1987*b*) until a best fit was obtained. The minimum number of components required for a fit was determined using the asymptotic information criterion (AIC) method (Akaike, 1974; Landaw and DeStefano, 1984). The autocorrelation

function was used to examine the correlation between the durations of successive openings or successive closings (Ball *et al.* 1985; Fredkin *et al.* 1985; Labarca *et al.* 1985; Kerry *et al.* 1987*a*,*b*).

Results

The longevity of patches obtained from the cultured myofibres was dependent upon the age of the cultures. With cultures maintained for less than 2 months *in vitro* giga-ohm seals were often unstable and the patches usually lasted only a few minutes. With cultures maintained for more than 3 months *in vitro* giga-ohm seals were less easy to obtain.

In preliminary studies, it was found that there was no difference in the distribution of K^+ channels along the length of a cultured myofibre. However, throughout this study most membrane patches were obtained from the middle region of a myofibre. About 60 % of seals formed spontaneously upon contact between the patch pipette and the myofibre. The remainder were formed by applying a slight negative pressure to the patch pipette interior. K^+ channels were usually seen as soon as a seal was formed and were observed in almost 50 % of the patches that were obtained.

102 recordings of K^+ channel activity, each from a separate membrane patch, were analysed. Five types of K^+ channel were identified in cell-attached and excised membrane patches, and have been designated types 1–5. In each case the channel type was characterised with respect to its open-channel conductance and voltage-sensitivity. All five types of K^+ channel were operative in cell-attached patches at the resting membrane potential of the myofibre, i.e. at a pipette potential of 0 mV. Using the whole-cell recording mode the mean resting potential measured for the myofibres was -39 ± 7 mV ($\pm$S.D., N=42). Several pieces of evidence point to the K^+ selectivity of these channels. First, the reversal potential and conductances of the single-channel currents were unaffected by the Cl^- channel blocker picrotoxin (1 mmol l^{-1}) or by the substitution of SO_4^{2-} for Cl^- in the pipette and/or the bathing saline (Miller and Usherwood, 1988; Duce *et al.* 1988; Miller, 1988). Second, the reversal potential for the single-channel currents was shown to follow the K^+ reversal potential (E_K) as estimated using the Nernst equation for a pure K^+ electrode. For cell-attached patches the internal K^+ concentration was taken as 140 mmol l^{-1} (Leech, 1986). With the cultured muscle bathed in standard saline and the patch pipette containing a high-K^+ saline, E_K had an estimated value of -6 mV, which corresponded to a pipette potential of -33 mV. Elevation of the K^+ concentration in the bathing saline from the normal 10 to 95 mmol l^{-1} shifted the single-channel I–V relationships to the right, i.e. the currents reversed near to a pipette potential of -20 mV. When the muscle was bathed in the high-K^+ saline (180 mmol l^{-1} K^+) the currents reversed near to a pipette potential of 0 mV (N=33). The type 1 and type 2 K^+ channels were observed most frequently, accounting for about 90 % of the channels seen in both cell-attached and excised patches.

The type 1 K^+ channel

The type 1 K^+ channel was that most frequently observed. Recordings from twenty-one cell-attached, two outside-out and four inside-out patches containing type 1 channels were analysed. The *I–V* relationship for this channel in cell-attached patches was non-linear with marked inward rectification. From the *I–V* curve of Fig. 1A,B, estimated chord conductances of 43 pS for inward current over the pipette potential (V_{pip}) (range +100 mV to −40 mV) and 8 pS for outward current between −40 mV and −60 mV are obtained. The channel current reversed at a pipette potential of −40 mV (an approximate membrane potential of 0 mV), which was close to E_K. Only outward currents were observed for the type 1 channel in excised, outside-out patches, to give a chord conductance of 5 pS between pipette potentials of 0 mV and +120 mV. In inside-out patches, only inward currents were observed, to give a chord conductance of 20 pS between pipette potentials of +40 mV and +100 mV. There was no evidence of subconductance states in any of the recordings of type 1 channel currents. Block of the type 1 channel currents by Ba^{2+}, 20 mmol l^{-1} in the pipette saline, was not observed.

In Fig. 1C, $\ln[(1-P_o)/P_o]$ for the type 1 channel is plotted as a function of applied pipette potential (V_{pip}). The values of P_o were obtained by pooling data from twenty-one cell-attached patches. From this plot $E_{1/2}$ was calculated to be a pipette potential of −120 mV, which corresponded to a membrane potential of +80 mV, and z was calculated to be −0.4. P_o became progressively larger as the pipette potential was made more negative (Fig. 1D). Thus, the increase in P_o as V_{pip} was made more negative could result in the total current flow through the channel being ohmic, despite the obvious inward rectification indicated by the *I–V* relationship. To test this idea, the single-channel current at each V_{pip} was multiplied by P_o and the product was plotted as a function of the V_{pip}. This showed that the relationship between the total current flowing through the type 1 K^+ channel and V_{pip} was not linear, but that P_o was considerably higher for all negative pipette potentials than for positive pipette potentials. P_o did not increase further when patches were excised (inside-out or outside-out for a variety of pipette potentials) into the bathing saline, which contained 2 mmol l^{-1} Ca^{2+}.

Most recordings of type 1 channels were too brief to enable a rigorous dwell time analysis to be undertaken. However, in one long-duration recording from a cell-attached patch, which appeared to contain only one channel, 2687 transitions between closed and open states were observed. The closed time PDF for these data was best fitted by the sum of four exponentials (Fig. 2A); the open time PDF was best-fitted by the sum of three exponentials (Fig. 2B). Autocorrelation function analysis of the channel closed times produced significant correlation, but the autocorrelation function for the open times showed that these were not correlated (Fig. 2C,D).

The type 2 K^+ channel

Recordings of type 2 K^+ channel currents obtained from twenty-four cell-

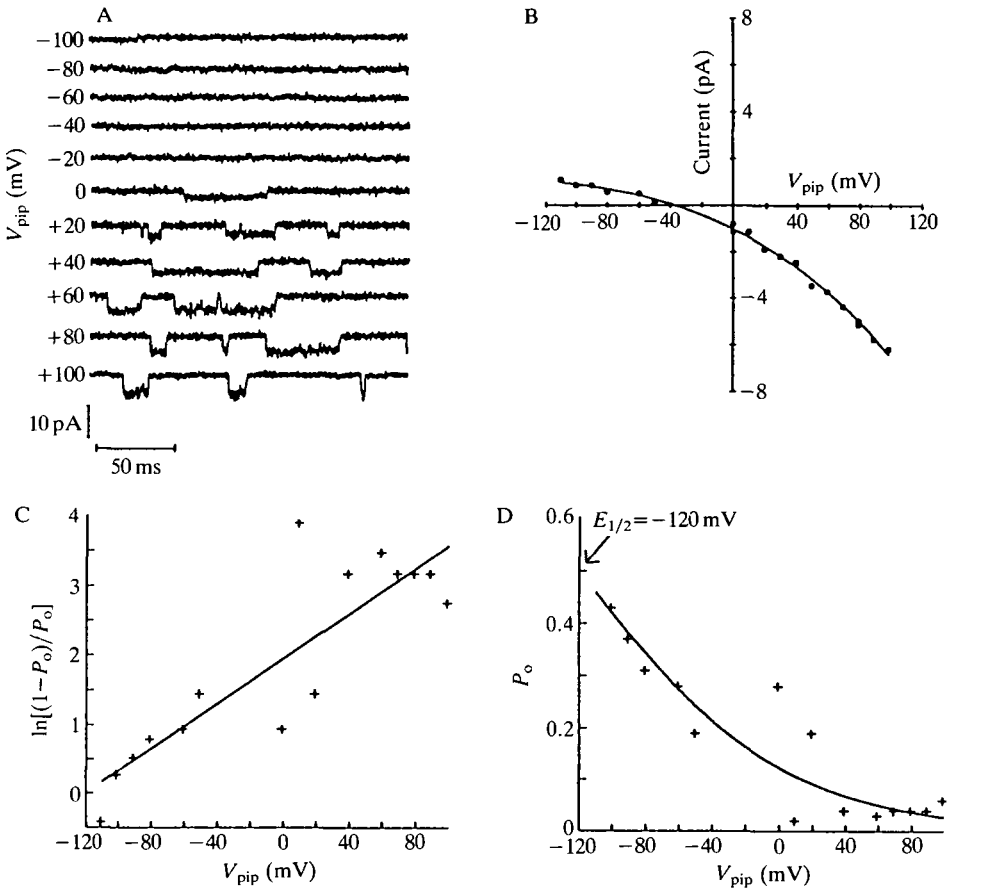

Fig. 1. (A) Records of type 1 K^+ channel currents made from a cell-attached patch at various pipette potentials (V_{pip}). The currents were low-pass filtered at a cut-off frequency of 3 kHz and digitised at 50 μs per point. (B) *I–V* relationship for the type 1 K^+ channel constructed from the data shown in A exhibits inward rectification. The channel current reversed at a V_{pip} of approximately −40 mV, which is near E_K. For values of V_{pip} less than −40 mV the channel current was outward. The chord conductance, measured between V_{pip} values of −40 mV and −100 mV was 8 pS. With values of V_{pip} greater than −40 mV the current was inward. The chord conductance between V_{pip} values of −40 mV and +100 mV was 43 pS. (C,D) The effect of V_{pip} on P_o for the type 1 K^+ channel. Data pooled from 21 cell-attached patches. (C) Linear regression of $\ln[(1-P_o)/P_o]$ *versus* V_{pip} allows an estimation of the gating charge z and $E_{1/2}$. The slope of the regression line is $-ze/KT$ and the intercept is $zE/KTE_{1/2}$. The value of $E_{1/2}$ can be converted from a V_{pip} to a true membrane potential by subtracting the calculated V_{pip} from the resting membrane potential. (D) Voltage-dependence of type 1 channel gating. The plot was fitted using a modification of the Boltzmann equation: $P_o=1/\{1+\exp[(w-zeE)/KT]\}$.

attached, nine outside-out and five inside-out patches were analysed. The type 2 channel currents exhibited inward rectification in cell-attached patches (Fig. 3), with a chord conductance of 115 pS for pipette potentials between +100 mV and

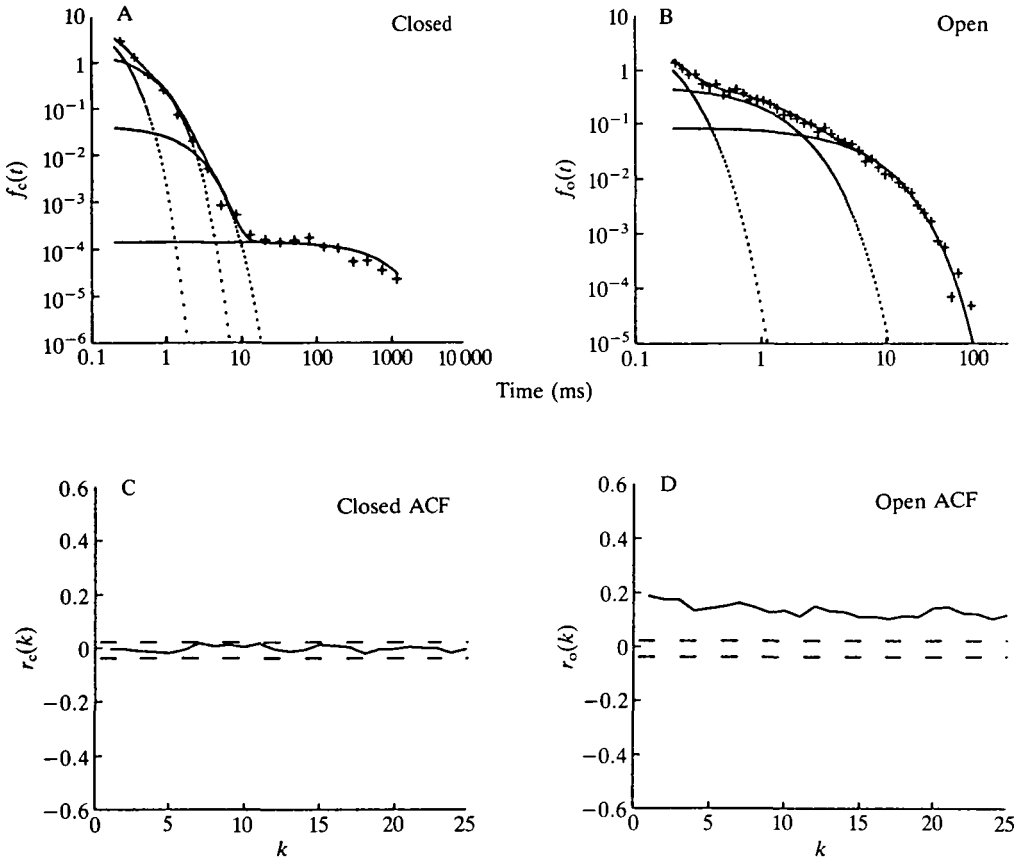

Fig. 2

−35 mV and 29 pS for pipette potentials between −30 mV and −100 mV. The channel current reversed at a pipette potential of −35 mV (a membrane potential of approximately −5 mV) which was near to the estimated E_K. In two cell-attached patches, subconductance states one-quarter, half and three-quarters of the amplitude of the full conductance level were seen. These subconductance states occurred in isolation, as well as preceding or following transitions to the full conductance state of the channel. Only outward currents were observed in outside-out patches. Between pipette potentials of 0 mV and +100 mV a chord conductance of 11 pS was obtained. In inside-out patches, the channel currents exhibited inward rectification, with a chord conductance of 28 pS between pipette potentials of −140 mV and −70 mV and 38 pS between −70 mV and +60 mV.

Type 2 channel activity consisted of bursts of brief openings interrupted by periods of inactivity. Because of the fast kinetics of this channel and the problem of recording bandwidth-limitation, no attempt was made to measure the dwell times for this channel. P_o for this channel was not altered when inside-out patches were excised into bathing saline containing 2 mmol l^{-1} Ca^{2+}.

With 20 mmol l^{-1} Ba^{2+} in the pipette saline there was clear evidence of channel block in cell-attached patches (Fig. 4). Both outward and the inward currents were

Fig. 2. Dwell time probability density functions (PDFs) provide information concerning the number of closed (N_c) and open (N_o) states of the channel. Closed time PDFs consist of N_c exponential terms, open time PDFs of N_o terms. The PDFs are given by the equations:

$$f_o(t) = \sum_{i=1}^{N_o} \alpha_i/\tau_i \exp(-t/\tau_i),$$

$$f_c(t) = \sum_{i=1}^{N_c} \alpha_i/\tau_i \exp(-t/\tau_i),$$

where $f_o(t)$ is the frequency of open times, $f_c(t)$ is the frequency of closed times, α_i is the proportion of the component i and τ_i is the time constant of the component i. The autocorrelation function (ACF) examines the correlation between successive openings or successive closings in relation to their dwell times. The ACF for the open times $[t_o(i)]$ and the closed times $[t_c(i)]$ are given by the following equations:

$$r_o(k) = \text{cov}[t_o(i), t_o(i+k)]/\text{var}[t_o(i)],$$

$$r_c(k) = \text{cov}[t_c(i), t_c(i+k)]/\text{var}[t_c(i)],$$

where $r_o(k)$ is the open time autocorrelation at lag k, $r_c(k)$ is the closed time autocorrelation at lag k, cov is the covariance of successive dwell times and var is the variance of successive dwell times. Probability functions (PDFs) of type 1 K^+ channel dwell times. The data were low-pass filtered at a cut-off frequency of 3 kHz and digitised at 20 μs per point. The dwell time PDFs were based on the measurement of 2687 events. (A) The closed time PDF was best fitted by the sum of four exponential components; the values of the time constants (τ) for these components are 0.12, 0.48, 1.70 and 755.9 ms. (B) The open time PDF was best fitted with three exponential components; the τ values being 0.08, 0.97 and 5.65 ms. (C,D) Autocorrelation function analysis of the channel closed times (C) and open times (D). The two horizontal dashed lines represent the 95 % confidence limits of $-3.72\times10^{-4}\pm0.0356$.

affected by Ba^{2+}, although inward currents were more affected than outward currents.

The following procedure was employed to determine whether the type 2 channel was ATP-sensitive. An inside-out patch containing at least one type 2 channel was held at a pipette potential of −90 mV. Single-channel currents were recorded from this patch prior to its perfusion with standard saline containing 1 mmol l^{-1} ATP (Fig. 5). Within a few seconds of ATP perfusion the channel activity declined to zero. The ATP was then removed by washing the patch with standard saline. After ATP removal, channel activity was at a much higher level than before, with two channels now being active in the membrane patch. Similar results were obtained with three separate inside-out membrane patches. The appearance of two channel openings after wash-out may represent some form of post-inhibitory activation of the type 2 K^+ channels (Findlay and Dunne, 1986).

The type 3 K^+ channel

Recordings of type 3 K^+ channel activity obtained from eight cell-attached, nine outside-out and four inside-out patches were analysed. In cell-attached patches the

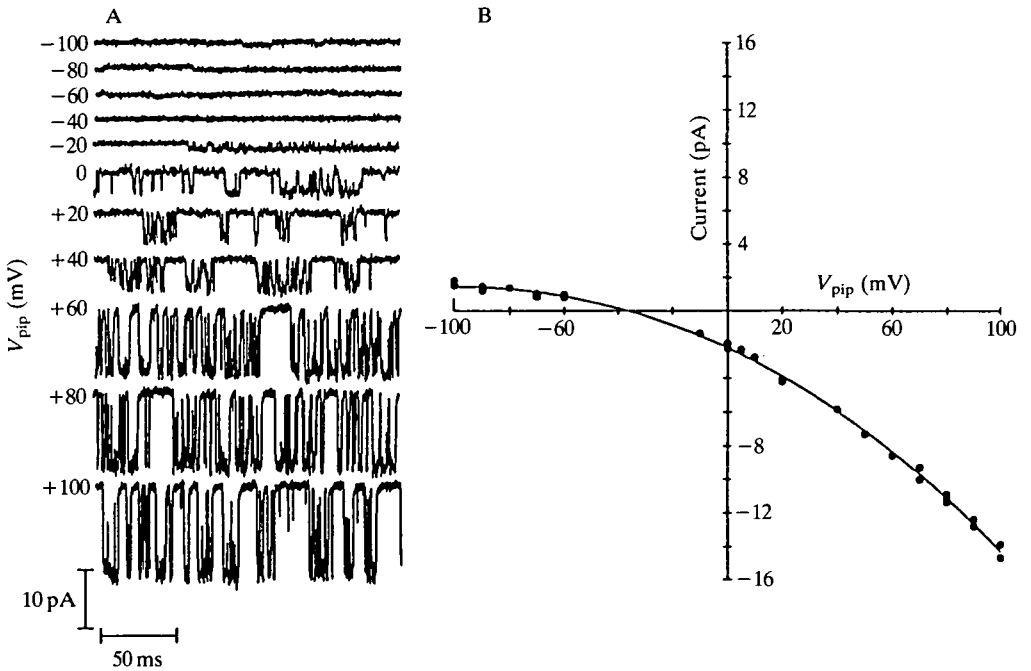

Fig. 3. (A) Recordings of type 2 K^+ channel currents made from a cell-attached patch. The data were low-pass filtered at a cut-off frequency of 3 kHz and digitised at 50 μs per point. (B) The *I–V* relationship in A indicates inward rectification. The channel currents reversed close to the estimated E_K. The channel had a chord conductance of 115 pS for inward currents, measured between V_{pip} values of −35 mV and +100 mV, and of 29 pS for outward currents, between V_{pip} values of −35 mV and −100 mV.

I–V relationship for this channel was linear, with a conductance of 130 pS (Fig. 6A,B). The channel current reversed at a V_{pip} of −30 mV (a membrane potential of −10 mV), which was close to the estimated E_K. Gating of the type 3 channel was voltage-dependent. In cell-attached patches, z was estimated to be −0.33 and $E_{1/2}$ to be +80 mV (V_{pip} −119 mV), respectively (Fig. 6C,D). The type 3 channel was sensitive to Ca^{2+}. In cell-attached patches it exhibited only very brief openings, i.e. P_o was low, but in excised patches (inside-out) bathed in standard locust saline containing 2 mmol l^{-1} Ca^{2+}, P_o was markedly higher. The type 3 channel was not blocked by 20 mmol l^{-1} Ba^{2+}, in the pipette saline.

It was observed during the course of these experiments that the type 3 channel was sensitive to stretching of the membrane patch: the channel activity increased with suction. However, this stretch-activation was not followed up experimentally.

Only outward currents were observed in outside-out patches. The *I–V* relationship showed rectification and gave a maximum slope conductance of 135 pS (Fig. 7A,B). Single-channel currents recorded from outside-out patches exhibited subconductance states one-quarter, half and three-quarters of the amplitude of the full conductance level (Fig. 7C,D). Dwell time PDFs were fitted

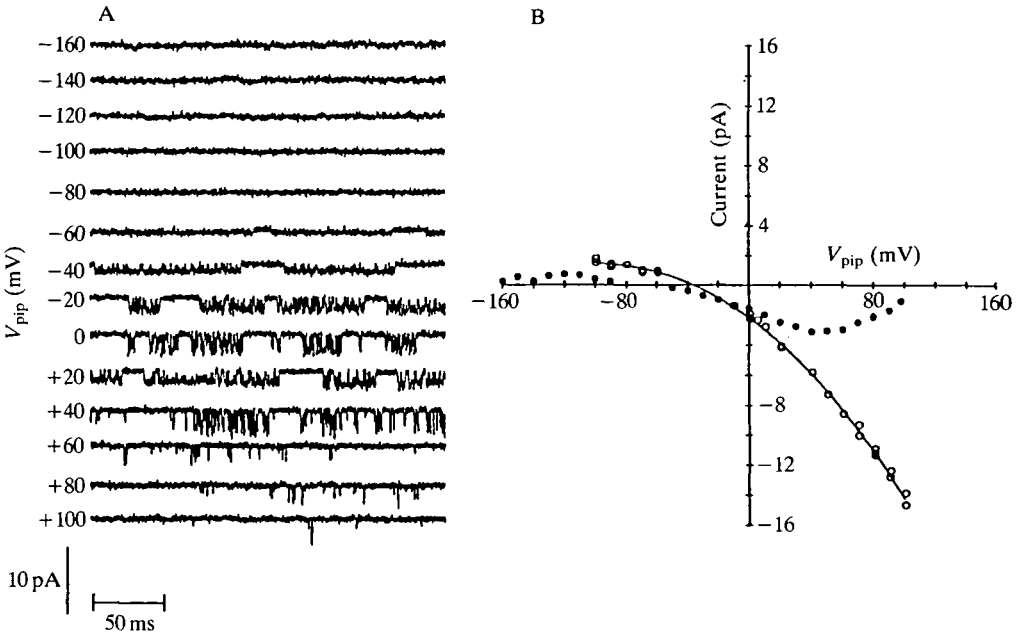

Fig. 4. (A) Type 2 K^+ channel currents recorded from a cell-attached patch, with 20 mmol l^{-1} Ba^{2+} in the patch pipette saline. (B) *I–V* relationships in the absence of Ba^{2+} (○) and in the presence of 20 mmol l^{-1} Ba^{2+} (●).

to data obtained from a recording of type 3 channel currents made from an outside-out patch held at a range of pipette potentials. The closed time PDFs constructed from these data were best fitted with three exponentials and the open time PDFs were best fitted by two exponentials (Table 1). As the pipette potential was made more positive the channel exhibited longer closings. The PDFs for 12 391 close–open transitions recorded at a pipette potential of +40 mV are shown in Fig. 8A,B. Significant correlations were found between successive openings and successive closings (Fig. 8C,D). In inside-out patches, the type 3 channel had a maximal chord conductance of 75 pS and the channel currents reversed at a pipette potential of −70 mV.

The type 4 K^+ channel

Nine recordings containing the type 4 K^+ channel, seven from cell-attached patches and two from inside-out patches, were obtained. This channel was not observed in outside-out patches. In cell-attached patches the *I–V* relationship for the type 4 channel was linear, with a conductance of 207 pS (Fig. 9). The channel current reversed at a pipette potential of −30 mV (a membrane potential of 0 mV), which was near to E_K. The channel exhibited a subconductance state which was three-quarters of the amplitude of the full conductance level. Estimates of $E_{1/2}$ and z are +22 mV (V_{pip} −62 mV) and −0.61, respectively. The type 4 channel

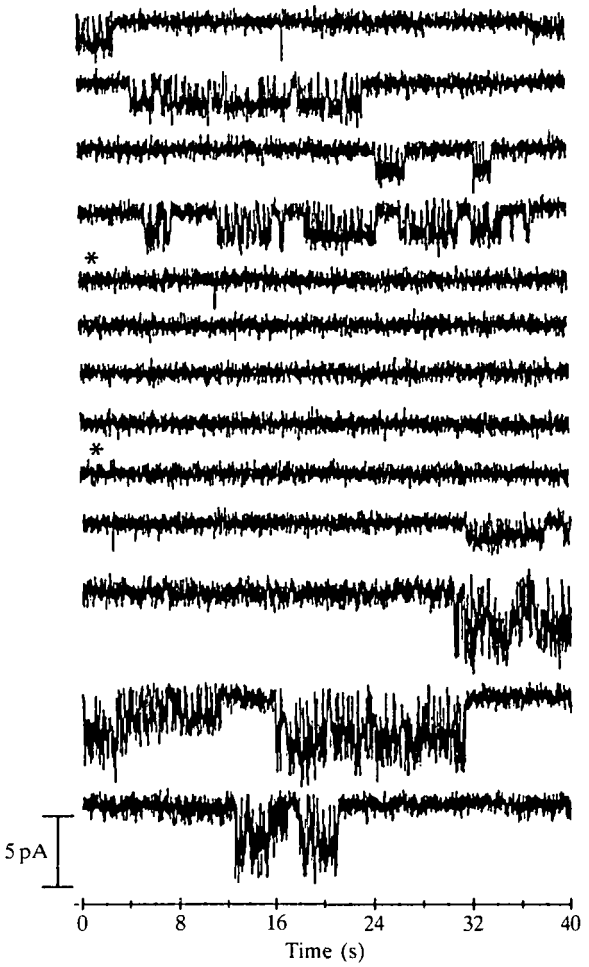

Fig. 5. The effect of ATP (1 mmol l^{-1}) on an inside-out membrane patch containing a type 2 K^+ channel. The patch was held at a V_{pip} of −90 mV. The first asterisk marks the introduction of ATP into the bath saline and the second one its subsequent wash-out with ATP-free saline.

exhibited little voltage-dependency, it was not Ca^{2+}-dependent and did not appear to be blocked by 20 mmol l^{-1} Ba^{2+} present in the pipette saline.

In inside-out patches the type 4 channel had a maximum conductance of 140 pS. Fig. 10A,B shows the dwell time PDFs for data obtained from an inside-out patch held at a pipette potential of −120 mV. The closed time PDF was best fitted by the sum of three exponential components. The open time PDF was best fitted by a single exponential. There was little correlation between successive closings, but there was significant correlation between successive openings (Fig. 10C,D).

The type 5 K^+ channel

This channel was observed only in cell-attached patches. The *I–V* relationship

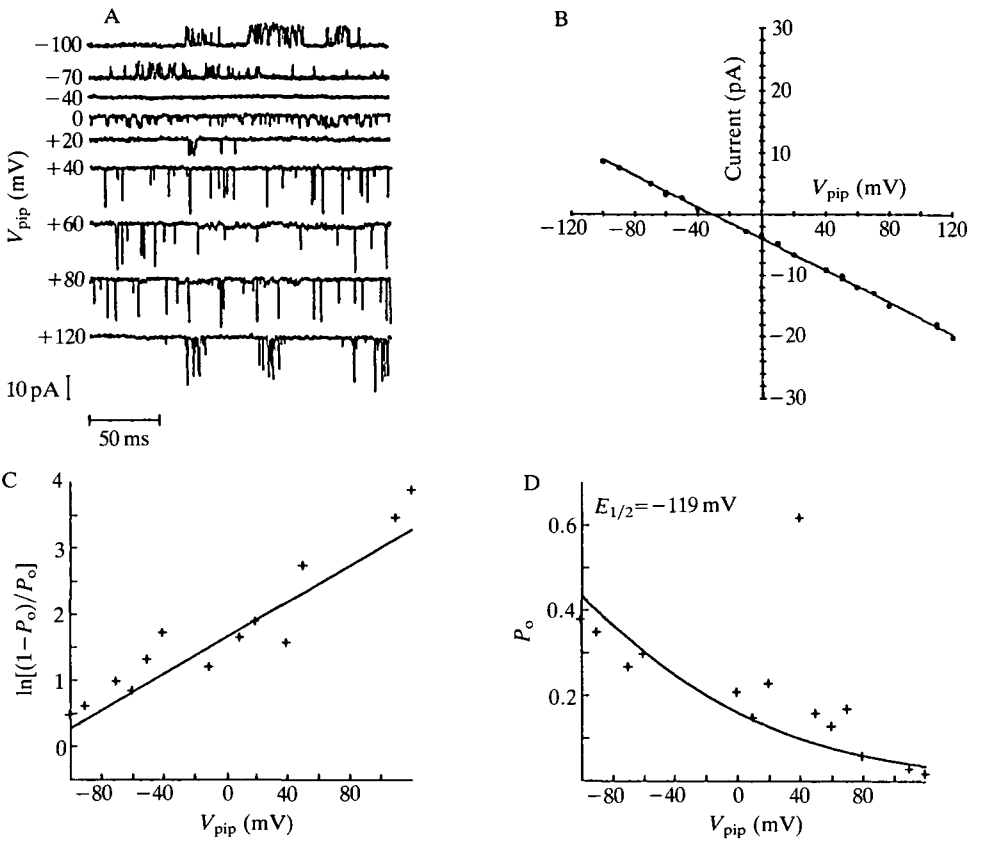

Fig. 6. (A) Type 3 K^+ channel currents recorded from a cell-attached patch. The data were low-pass filtered at a cut-off frequency of 3 kHz and digitised at 50 μs per point. (B) *I–V* relationship for a type 3 channel. The single-channel conductance estimated from the slope of the relationship was 130 pS. The channel current reversed at a V_{pip} of −30 mV, which was near E_K. (C,D) The effects of V_{pip} on P_o of a type 3 K^+ channel in a cell-attached patch. (C) Linear regression of $\ln[(1-P_o)/P_o]$ *versus* V_{pip}. (D) P_o plotted as a function of V_{pip}.

for the type 5 K^+ channel was curvilinear (Fig. 11), with a maximal slope conductance of 5 pS. This channel appeared to be an inward rectifier. Because of the poor signal-to-noise ratio, the reversal potential for the channel current could not be determined accurately.

Discussion

The results presented here demonstrate that five types of K^+ channel co-exist in cultured embryonic locust muscle. There appeared to be three inward rectifiers, the type 1, type 2 and type 5 channels, and two channels with large linear conductances, the type 3 and type 4 channels. The presence of inward rectifiers in

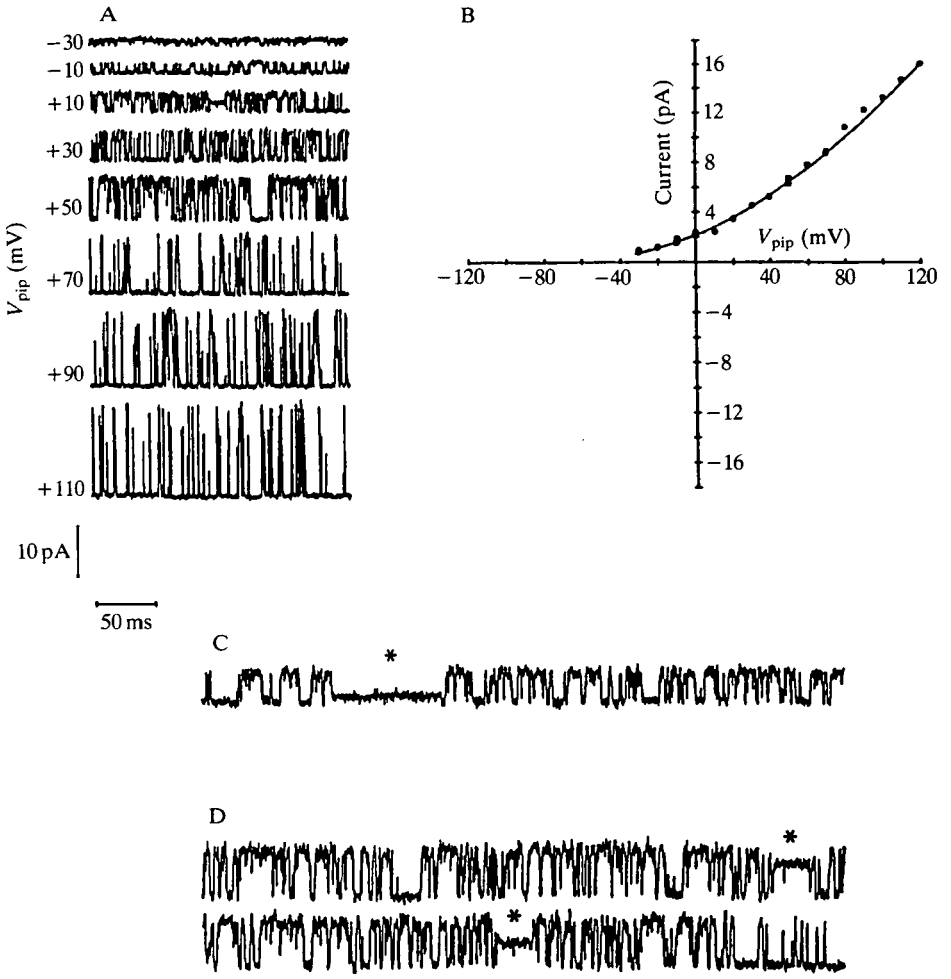

Fig. 7. (A) Type 3 K^+ channel currents recorded from an outside-out patch. Note the appearance of a subconductance state (*) at V_{pip} +10 mV. (B) An I–V relationship for the type 3 K^+ channel shown in A. (C,D) Subconductance states of a type 3 K^+ channel recorded from an outside-out patch. (C) A subconductance state (*) of one-quarter the amplitude of the full conductance level. In D the first trace shows a subconductance state (*) three-quarters of the amplitude of the full conductance state, whilst in the second trace the sub-state (*) is half that of the full state. The recordings in A, C and D were low-pass filtered at a cut-off frequency of 3 kHz and digitised at 50 μs per point.

this preparation was not surprising, since an inwardly rectifying current is present in adult locust muscle (Usherwood, 1969). The apparent lack of a delayed rectifier channel is surprising, especially since excitatory postsynaptic potentials and spontaneous contractions of the myofibres have been reported previously (Miller, 1988). However, this may reflect the developmental stage of the cultured

Table 1. *Parameter (α_i and τ_i) estimates for the closed time PDFs obtained for recordings of type 3 K^+ channel activity in an outside-out patch of locust muscle* in vitro

A. *Closed time PDFs*

V_{pip}	α_1	τ_1	α_2	τ_2	α_3	τ_3
0	0.29	0.11	0.42	0.56	0.29	1.32
+10	0.07	0.15	0.29	0.69	0.64	1.28
+20	0.16	0.13	0.18	0.41	0.66	0.99
+30	0.22	0.14	0.47	1.06	0.31	2.40
+40	0.17	0.15	0.56	1.26	0.27	3.05
+50	0.13	0.16	0.53	1.55	0.34	4.08
+60	0.15	0.15	0.51	1.14	0.34	2.34
+70	0.10	0.15	0.49	1.90	0.41	4.85

The closed time PDF is best fitted by three exponential components.

B. *Open time PDFs*

V_{pip}	α_1	τ_1	α_2	τ_2
0	0.13	0.30	0.87	1.22
+10	0.18	0.33	0.82	1.20
+20	0.19	0.34	0.81	0.98
+30	0.11	0.22	0.89	0.84
+40	0.58	0.54	0.42	0.96
+50	0.66	0.47	0.34	0.90
+60	0.32	0.43	0.68	0.83
+70	0.23	0.26	0.77	0.63

The open time PDF is best fitted by the two exponential components.

embryonic muscle where synaptic transmission may either be absent or at an early stage in its development.

There are few similarities between the K^+ currents in *Drosophila* muscle and those of the embryonic locust muscle. Both preparations have Ca^{2+}-sensitive K^+ currents, but the Ca^{2+}-dependent currents of *Drosophila* (I_{KCa} and I_{Acd}) rapidly inactivate and are blocked by Ba^{2+} (Wu and Ganetzky, 1988), whereas the Ca^{2+}-sensitive type 3 channel of locust muscle does not inactivate and is not blocked by Ba^{2+}. Both preparations have a large-conductance, stretch-sensitive channel, but the *Drosophila* K_{ST} channel is a Ca^{2+}-insensitive, voltage-independent channel (Zagotta *et al.* 1988) and the locust type 3 channel is Ca^{2+}-sensitive and voltage-dependent. Rapidly activating and inactivating K^+ channels, such as those responsible for the I_A current of *Drosophila*, are unlikely to have been seen with the experimental method employed. Patch pipette holding potentials were shifted manually, not by voltage-jumps, so any transient voltage-sensitive channel present would probably have inactivated during the time taken to alter the membrane potential.

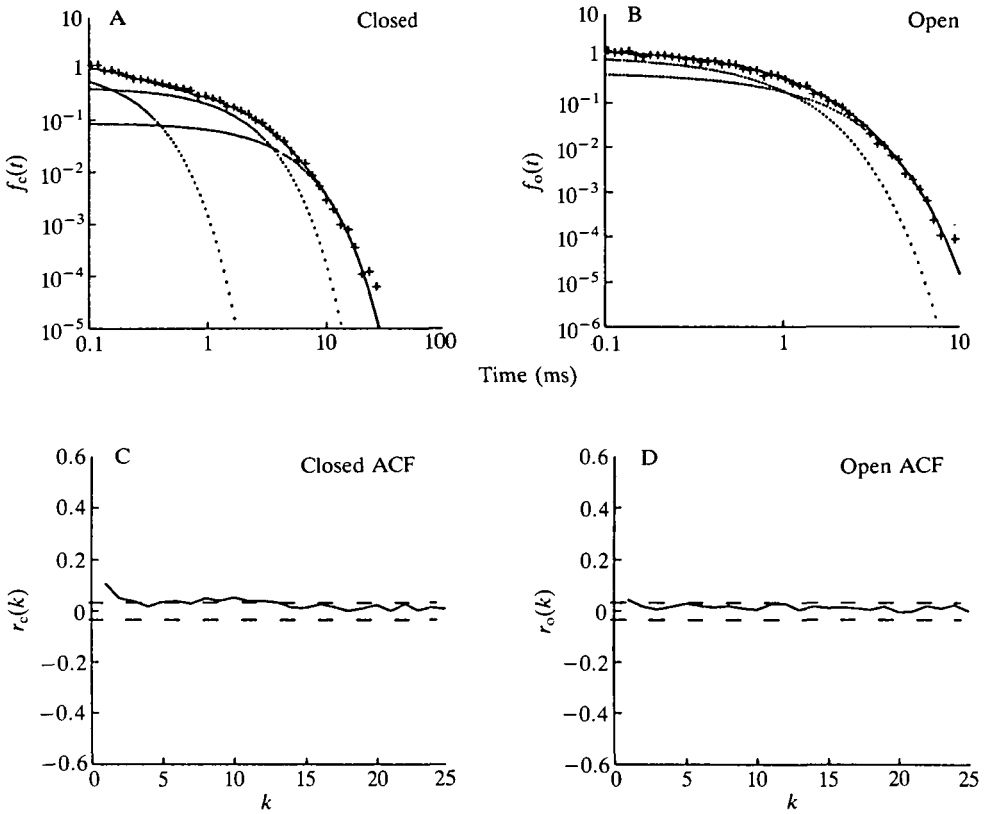

Fig. 8. Dwell time PDFs for type 3 K^+ channel currents recorded from an outside-out patch held at a V_{pip} of +40 mV. 12 391 close-open transitions were measured. The data were low-pass filtered at 10 kHz and digitised at 20 μs per point. (A) Closed time PDF best fitted with three exponentials; the values of the time constant (τ) are 0.15, 1.26 and 3.05 ms. (B) Open time PDF best fitted with two exponentials; the τ values are 0.54 and 0.96 ms. Autocorrelation function (ACF) analysis for the closed (C) and open (D) times showing weak correlation. The dashed lines represent the 95 % confidence limits of $-8.07\times10^{-5}\pm0.0180$.

P_o for the types 1 and 3 K^+ channels was voltage-dependent, whereas P_o for the type 4 channel appeared to be voltage-independent. It was not possible to measure P_o for channel types 2 and 5, but for both of these channels the open times appeared to shorten with hyperpolarisation. All the channels had a P_o above zero at the resting potential of the myofibre. The values for $E_{1/2}$ were as follows: type 1, +80 mV; type 3, +80 mV; and type 4, +22 mV. Using a simple two-state model, the constant voltage-dependence for the type 1, 3 and 4 channels could be accounted for by a Boltzmann-type equilibrium function with values for z of −0.40, −0.33 and −0.61, respectively. Reported values of z range from 0.40 for Ca^{2+}-activated K^+ channels in human red blood cells to 1.00 for the rabbit sarcoplasmic reticulum K^+ channel (Moczydlowski, 1986). The types 2 and 3

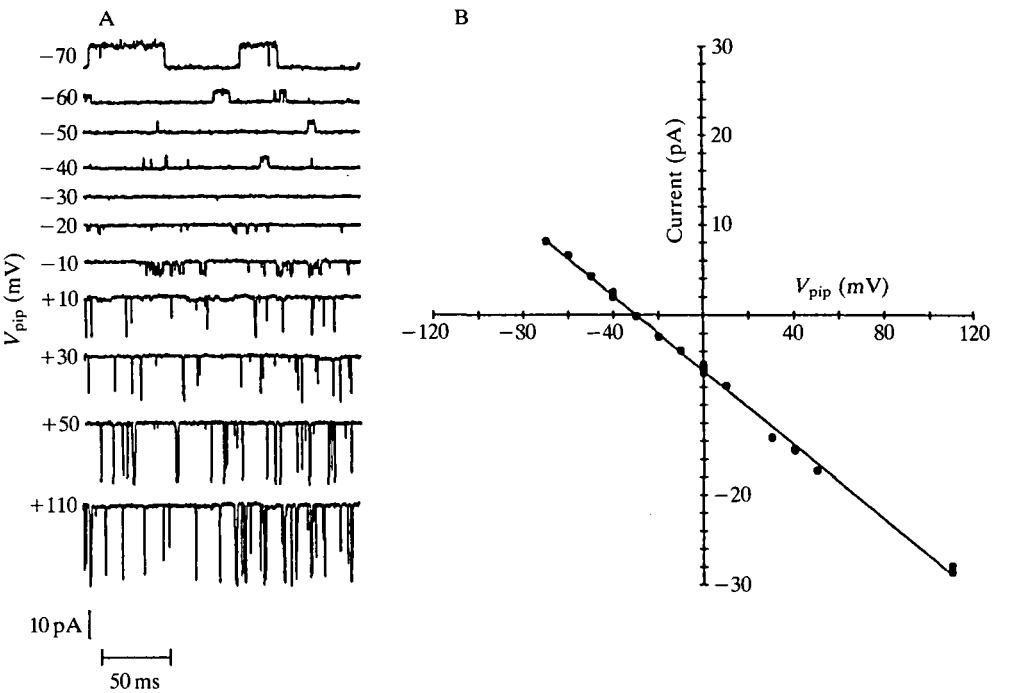

Fig. 9. (A) Type 4 K^+ channel currents recorded in a cell-attached patch at different values of V_{pip}. The data were low-pass filtered at a cut-off frequency of 3 kHz and digitised at 50 μs per point. (B) I–V relationship for channel currents shown in A. The single-channel conductance estimated from the slope of the relationship was 207 pS. The reversal potential at a V_{pip} of −30 mV was near to E_K.

channels appear to be driven by chemical modulators, the type 2 channel by ATP and the type 3 channel by Ca^{2+}.

Dwell time analysis for the type 1, type 3 and type 4 channels revealed multiple closed and open states, with the autocorrelation functions having values greater than zero. This suggests that the gating of these channels may be best described by branched or cyclic models rather than by simple linear systems. No attempt has yet been made to fit models to these data.

Our results are not sufficient to allow precise physiological roles to be ascribed to each channel type. We can only speculate about their contribution to the total current record. The type 1 and type 2 inward rectifiers accounted for about 90 % of the channels observed. These channels may be involved in the long-term regulation of the resting membrane conductance. However, the type 5 inward rectifier channel was not as ubiquitous and was of such low conductance that it would be unlikely to contribute substantially to the resting conductance. In fact, it is difficult to postulate what role a channel such as the type 5 channel would have. The Ca^{2+}-sensitive type 3 channel may serve to repolarise or even hyperpolarise the cell during periods of raised internal free Ca^{2+} concentration. Perhaps depolarisation of the myofibre membrane leads to an increase in its Ca^{2+}

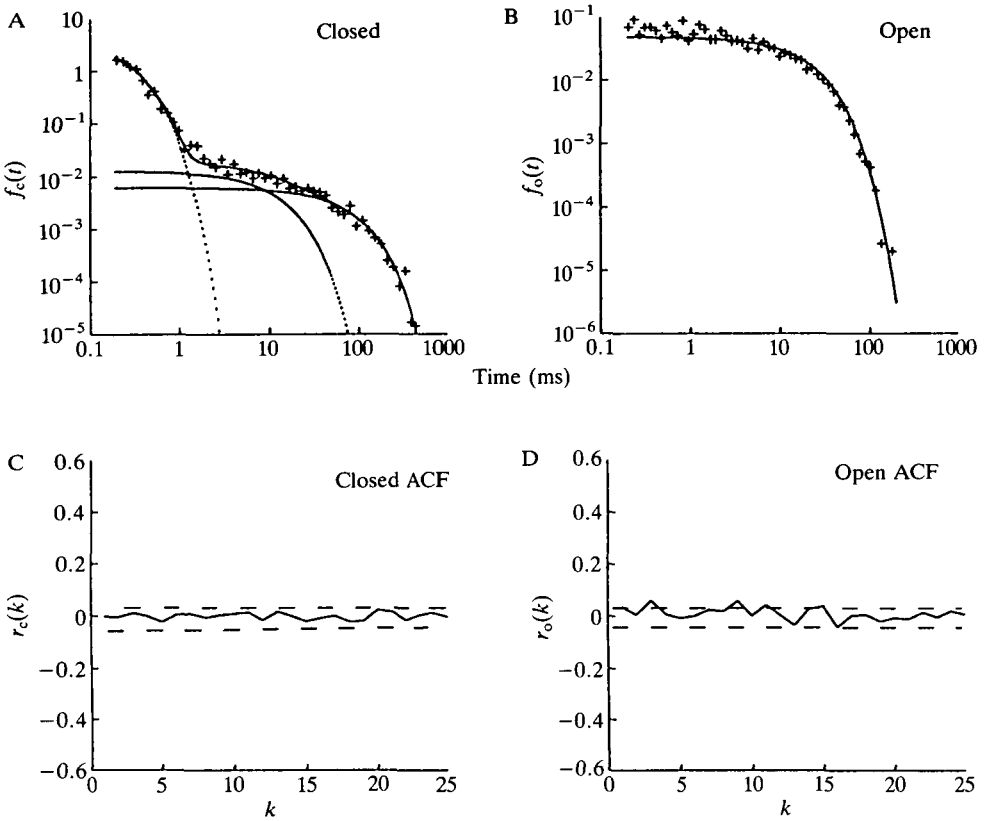

Fig. 10. Dwell time PDFs for type 4 K^+ channel currents recorded from an inside-out patch at a V_{pip} of −120 mV. The data were low-pass filtered at a cut-off frequency of 10 kHz and digitised at 20 μs per point. 1992 events were measured. (A) Closed time PDF was best fitted with three exponential components; the values of the time constant (τ) are 0.13, 2.65 and 14.13 ms. (B) Open time PDF best fitted using a single exponential; the τ value is 51.62 ms. (C) Closed time autocorrelation function (ACF), showing no significant correlations, and (D) open time ACF, showing weak correlations. The dashed lines represent the 95 % confidence limits of $-5.02\times10^{-4}\pm0.0448$.

permeability, as it does in adult locust skeletal muscle (Usherwood, 1969); such an occurrence would certainly activate type 3 channels. Additionally, the stretch-sensitivity of the type 3 channel suggests that this channel may also be involved in regulating membrane excitability during contractions of the myofibre. A K^+ channel with similar properties to the type 4 K^+ channel has been observed in cell-attached patches on adult locust muscle (Huddie *et al.* 1986). In the same preparation, a large proportion of the membrane conductance at the resting potential can be accounted for by an ohmic K^+ conductance, which is reduced by FMRFamide-like peptides and proctolin in a G-protein-dependent manner (Walther and Zittlau, 1989; Zittlau *et al.* 1989).

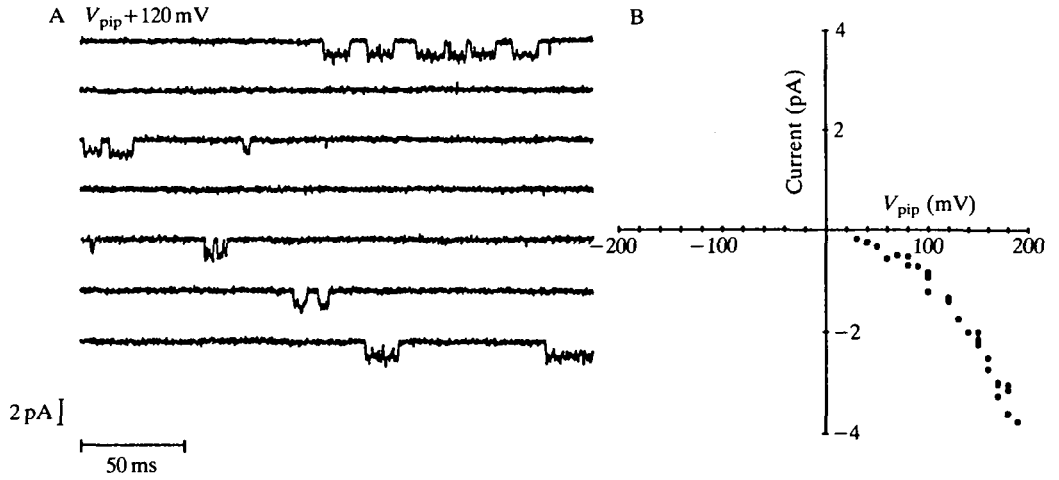

Fig. 11. (A) Single-channel currents recorded from a type 5 K^+ channel in a cell-attached patch held at a V_{pip} of +120 mV. The data were low-pass filtered at a cut-off frequency of 3 kHz and digitised at 50 μs per point. (B) *I–V* relationship for the type 5 K^+ channel. Extrapolation of the relationship to zero channel current gives an estimated reversal potential of V_{pip} −30 mV. The maximal slope conductance is 5 pS.

We are grateful to Dr C. F. Walther for his comments on the manuscript, and to Drs R. L. Ramsey and M. S. P. Sansom for the provision of computer programs. This work was funded by the British Science and Engineering Research Council.

References

AKAIKE, H. (1974). A new look at the statistical model identification. *IEEE (Inst. Elect. Electron. Eng.) Trans. Autom. Control.* **AC19**, 716–723.

BALL, F. G. AND SANSOM, M. S. P. (1987). Temporal clustering of ion channel openings incorporating time interval omission. *IMA (Inst. Math. Appl.) J. math. med. Biol.* **4**, 333–361.

BALL, F. G. AND SANSOM, M. S. P. (1988). Aggregated Markov processes incorporating time interval omission. *Adv. appl. Prob.* **20**, 546–572.

BALL, F. G., SANSOM, M. S. P. AND USHERWOOD, P. N. R. (1985). Clustering of glutamate receptor-channel openings recorded from the locust (*Schistocerca gregaria*) muscle. *J. Physiol., Lond.* **360**, 66P.

BLATZ, A. L. AND MAGLEBY, K. L. (1986). Quantitative description of three modes of activity of fast chloride channels from rat skeletal muscle. *J. Physiol., Lond.* **378**, 141–174.

CHEN, J. S. AND LEVI-MONTALCINI, R. (1969). Axonal outgrowth and cell migration *in vitro* from nervous system of cockroach embryos. *Science* **166**, 631–632.

COLQUHOUN, D. AND SIGWORTH, F. (1983). Fitting and statistical analysis of single-channel records. In *Single Channel Recording* (ed. B. Sakmann and E. Neher), pp. 191–263. New York: Plenum Press.

DUCE, J. A., MILLER, B. A. AND USHERWOOD, P. N. R. (1988). Patch clamp studies of cultured muscle from locust embryos. In *Cell Culture Approaches to Invertebrate Neuroscience* (ed. D. J. Beadle, G. Lees and S. B. Kater), pp. 221–233. London: Academic Press.

DUCE, J. A. AND USHERWOOD, P. N. R. (1986). Primary cultures of muscle from embryonic locusts (*Locusta migratoria*, *Schistocerca gregaria*): developmental, electrophysiological and patch-clamp studies. *J. exp. Biol.* **123**, 307–323.

FINDLAY, I. AND DUNNE, M. J. (1986). ATP maintains ATP-inhibited K^+ channels in an operational state. *Pflügers Arch.* **407**, 238–240.

FREDKIN, D. R., MONTAL, M. AND RICE, J. A. (1985). Identification of aggregated Markovian models: Application to the nicotinic acetylcholine receptor. In *Proceedings of the Berkeley Conference in Honour of Jerzy Neyman and Jack Kiefer* (ed. L. M. LeCan and R. A. Ohlsen), pp. 269–289. Wadsworth Publishing Co., Belmont.

HAMILL, O. P., MARTY, A., NEHER, E., SAKMANN, B. AND SIGWORTH, F. J. (1981). Improved patch-clamp techniques for high-resolution current recording from cells and cell-free membrane patches. *Pflügers Arch.* **391**, 85–100.

HILLE, B. (1984). Ionic channels of excitable membranes. Sinauer Associates, Sunderland, Massachusetts, USA.

HUDDIE, P. L., RAMSEY, R. L. AND USHERWOOD, P. N. R. (1986). Single potassium channels of adult locust (*Schistocerca gregaria*) muscle recorded using the giga-ohm seal patch-clamp technique. *J. Physiol., Lond.* **378**, 60P.

KERRY, C. J., KITS, K. S., RAMSEY, R. L., SANSOM, M. S. P. AND USHERWOOD, P. N. R. (1987*a*). Single channel kinetics of a glutamate receptor. *Biophys. J.* **51**, 137–144.

KERRY, C. J., RAMSEY, R. L., SANSOM, M. S. P. AND USHERWOOD, P. N. R. (1987*b*). Glutamate receptor-channel kinetics: the effect of glutamate concentration. *Biophys. J.* **53**, 39–52.

KERRY, C. J., RAMSEY, R. L., SANSOM, M. S. P., USHERWOOD, P. N. R. AND WASHIO, H. (1987*c*). Single-channel studies of the action of (+)-tubocurarine on locust muscle glutamate receptor. *J. exp. Biol.* **127**, 121–134.

KOLB, H. A. (1989). Potassium channels in excitable and non-excitable cells. *Rev. Physiol. Biochem. Pharmac.* (in press).

LABARCA, P. P., RICE, J. A., FREDKIN, D. R. AND MONTAL, M. (1985). Kinetic analysis of channel gating: application to the cholinergic receptor and the chloride channel from *Torpedo californica*. *Biophys. J.* **47**, 469–478.

LAMB, T. D. (1985). A digital tape-recorder suitable for fast physiological signals. *J. Physiol., Lond.* **360**, 5P.

LANDAW, E. M. AND DESTEFANO, J. J. (1984). Multiexponential, multicompartmental, and non-compartmental modelling. II. Data analysis and statistical considerations. *Am. J. Physiol.* **246**, R665–R677.

LATORRE, R. (1986). The large calcium-activated potassium channel. In *Ion Channel Reconstitution* (ed. C. Miller), pp. 431–467. Plenum Press, New York.

LATORRE, R. AND MILLER, C. (1983). Conduction and selectivity in potassium channels. *J. Membr. Biol.* **71**, 11–30.

LEECH, C. A. (1986). Resting potential and potassium-selective electrode measurements in locust skeletal muscles. *J. exp. Biol.* **122**, 439–442.

LUX, H. D., NEHER, E. AND MARTY, A. (1981). Single channel activity associated with the calcium dependent outward current in *Helix pomatia*. *Pflügers Arch.* **389**, 293–295.

MARQUADT, D. W. (1963). An algorithm for least-squares estimation of non-linear parameters. *J. Soc. indust. appl. Math.* **11**, 431–441.

MILLER, B. A. (1988). Potassium channels in cultured locust muscle. PhD thesis, University of Nottingham, UK.

MILLER, B. A. AND USHERWOOD, P. N. R. (1988). Potassium channels in cultured locust muscle. *Pesticide Sci.* **24**, 85–87.

MOCZYDLOWSKI, E. (1986). Single-channel enzymology. In *Ion Channel Reconstitution* (ed. C. Miller), pp. 75–113. New York: Plenum Press.

PICHON, Y. AND ASHCROFT, F. M. (1985). Nerve and muscle: Electrical activity. In *Comprehensive Insect Physiology, Biochemistry and Pharmacology*, vol. 5, *Nervous System: Structure and Motor Function* (ed. G. A. Kerkut and L. I. Gilbert), pp. 85–113. Oxford: Pergamon Press.

PIEK, T. AND NJIO, K. D. (1979). Morphology and electrochemistry of insect muscle fibre membrane. *Adv. Insect Physiol.* **14**, 185–249.

RUDY, B. (1988). Diversity and ubiquity of K^+ channels. *Neuroscience* **25**, 729–749.

SALKOFF, L. B. (1983). Genetic and voltage-clamp analysis of a *Drosophila* potassium channel. *Cold Spring Harb. Symp. quant. Biol.* **48**, 221–231.

SALKOFF, L. B. AND WYMAN, R. J. (1983). Ion currents in *Drosophila* flight muscle. *J. Physiol., Lond.* **337**, 687–709.

SHIELDS, G., DUBENDORFER, A. AND SANG, J. H. (1975). Differentiation *in vitro* of larval cell types from early embryonic cells of *Drosophila melanogaster*. *J. Embryol. exp. Morph.* **33**, 159–175.

SOLC, C. K., ZAGOTTA, W. N. AND ALDRICH, R. W. (1987). Single-channel and genetic analysis reveal two distinct A-type potassium channels in *Drosophila*. *Science* **236**, 1094–1098.

USHERWOOD, P. N. R. (1967). Permeability of insect muscle fibres to potassium and chloride ions. *J. Physiol., Lond.* **191**, 29P–30P.

USHERWOOD, P. N. R. (1969). Electrochemistry of insect muscle. *Adv. Insect Physiol.* **6**, 205–278.

USHERWOOD, P. N. R. AND GRUNDFEST, H. (1965). Peripheral inhibition in skeletal muscle of insects. *J. Neurophysiol.* **28**, 497–518.

WALTHER, C. AND ZITTLAU, K. E. (1989). Do YGGFMRF-amide and proctolin act on the same potassium conductance in locust skeletal muscle. *J. Physiol., Lond.* **410**, 32P.

WU, C.-F. (1988). Genetic and pharmacological analyses of potassium channels in *Drosophila*. *Pesticide Science*. In press.

WU, C.-F. AND GANETZKY, B. (1988). Genetic and pharmacology analyses of potassium channels in *Drosophila*. In *Neurotox '88, Molecular Basis of Drug and Pesticide Action* (ed. G. Lunt). Internal Congress Series 832. pp. 311–325.

WU, C.-F., GANETZKY, B., HAUGLAND, F. N. AND LIU, A. X. (1983). Potassium currents in *Drosophila*: Different components affected by mutations of two genes. *Science* **220**, 1076–1078.

ZAGOTTA, W. N., BRAINARD, M. S. AND ALDRICH, R. W. (1988). Single-channel analysis of four distinct classes of potassium channels in *Drosophila* muscle. *J. Neurosci.* **8**, 4765–4779.

ZITTLAU, K. E., MURCK, H. AND WALTHER, C. (1989). G-protein dependent action of proctolin and YGGFMRF-NH_2 on K^+-conductance in locust skeletal muscle. *Abstracts of the 12th Annual Meeting of the European Neuroscience Association, Turin.*